



Image Denoising Method Using curvelet Transform and Wiener Filter

A. Anilet Bala¹, Chiranjeeb Hati² and CH Punith³

Assistant professor, Dept. of ECE, SRM University, chennai, Tamilnadu, India¹

UG Student [ECE], Dept. of ECE, SRM University, chennai, Tamilnadu, India²

UG Student [ECE], Dept. of ECE, SRM University, chennai, Tamilnadu, India³

ABSTRACT: A new image denoising method based on curvelet transform is proposed. The limitations of commonly used separable extensions of one-dimensional transforms, such as the Fourier and wavelet transforms, in capturing the geometry of image edges are well known. Here, we pursue "true" two-dimensional transform that can capture the intrinsic geometrical structure that is key in visual information. Denoising of an image is done by processing an image through Wiener filter and using curvelet transform [1], [6]. Experimental results show that proposed denoising technique performs better in terms of the PSNR. We have compared PSNR values of proposed algorithm with that of wavelet and curvelet in RGB and YCbCr regions.

Keywords: curvelets, discrete wavelet transform, FFT, radon transform, ridgelets, Wiener filter.

I. INTRODUCTION

Visual perception has become an essential part of communication in today's world. Because of which it is important to ensure that transmitted data is not corrupted by any kind of unwanted signals called noise. Noises are generated due to the improper modelling of production and/or capturing system of the signal. Therefore, real world signals usually contain deviations from the ideal signal that is expected. Image denoising is an important pre-processing task for further image processing such as edge detection or image segmentation. The main aim of any denoising algorithm is to reduce noise levels, while preserving the image features. At present day, there are various image denoising algorithms available which are successful in denoising a noisy image, but are inefficient in attaining better signal to noise ratio and/or retaining the image features.

II. RELATED WORKS

Although the DWTs have established an impressive reputation as a tool for mathematical analysis and signal processing, it has the disadvantage of poor directionality, which has undermined its usage in many applications. Significant progress in the development of directional wavelets has been made in recent years. The complex wavelet transform have improved directional selectivity. However, the complex wavelet transform has not been widely used in the past, as it is difficult to design complex wavelets with perfect reconstruction properties and good filter characteristics. The dual-tree complex wavelet transform (DT CWT) proposed by Kingsbury [4], which added perfect reconstruction to the other attractive properties of complex wavelets.

The 2-D complex wavelets are essentially constructed by using tensor-product one-dimensional (1-D) wavelets. The directional selectivity provided by complex wavelets (six directions) is much better than that obtained by the classical DWTs (three directions), but is still limited.

In 1999, an anisotropic geometric wavelet transform, named ridgelet transform, was proposed by Candès and Donoho [6]. The ridgelet transform is optimal at representing straight-line singularities. Unfortunately, global straight-line singularities are rarely observed in real applications. To analyse local line or curve singularities, a natural idea is to consider a partition of the image, and then to apply the ridgelet transform to the obtained sub images. This block ridgelet-based transform, which is named curvelet transform, was first proposed by Candès and Donoho in 2000.

International Journal of Advanced Research in Electrical, Electronics and Instrumentation Engineering

(An ISO 3297: 2007 Certified Organization)

Vol. 3, Issue 1, January 2014

III. PROPOSED ALGORITHM

In this paper, we propose a novel denoising method. The method uses curvelet transform and Wiener filtering [8] to denoise an image. Initially we obtain a noisy image by degrading it by adding additive Gaussian noise (most common type of noise). Then we implement our algorithm, which firstly passes it through a Wiener filter. And then the output of which is then applied by curvelet transform. The resultant image is denoised and also retains the important image information. Fig.1 shows the flow of the proposed algorithm.

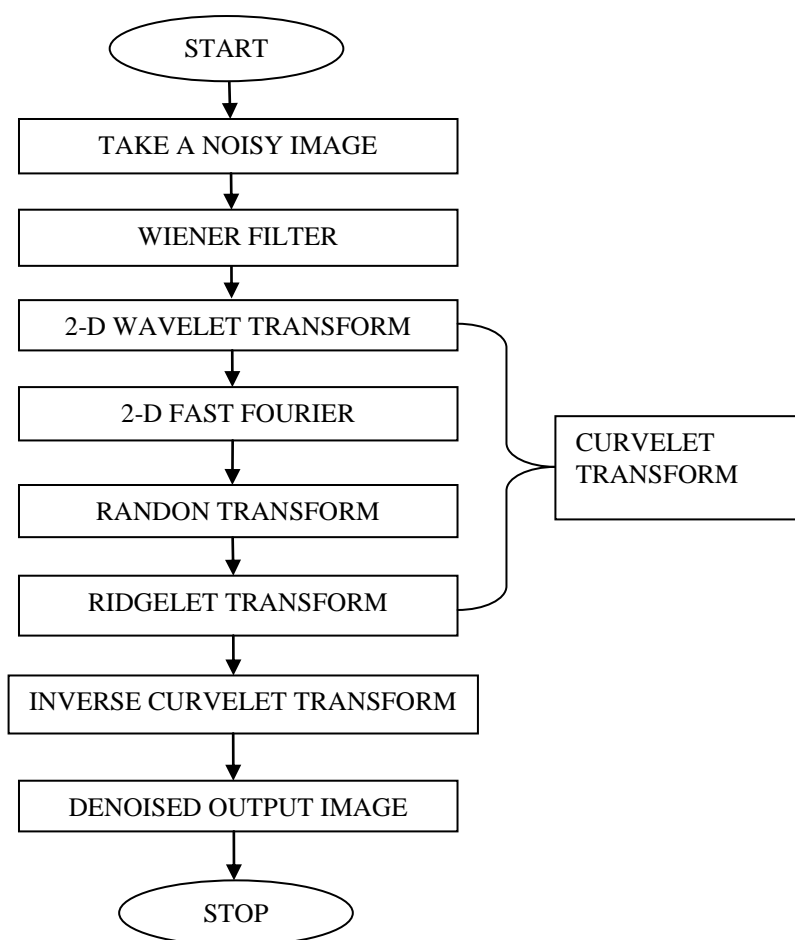


Fig.1. Proposed Algorithm

A. WIENER FILTERING

The Wiener filter is commonly utilized because of its simplicity and its speed. It is deemed simple because it uses a system of linear equations to calculate a set of optimal filter weights that reduce the noise level of a received signal. It estimates cross-correlation and covariance matrices of noisy signals to calculate these weights and provide an accurate Estimate of the undistorted deterministic signal under Gaussian noise. The noise statistics are estimated and then used to determine a set of optimal filter weights. By then processing a new input signal, containing similar noise characteristics, with the optimal filter weights, the signal deterministic component is estimated. This method is optimal when the noise distribution is Gaussian. Furthermore, its execution only requires a few computational steps that are very fast to process.



International Journal of Advanced Research in Electrical, Electronics and Instrumentation Engineering

(An ISO 3297: 2007 Certified Organization)

Vol. 3, Issue 1, January 2014

The inverse filtering is a restoration technique for deconvolution, i.e., when the image is blurred by a known lowpass filter, it is possible to recover the image by inverse filtering or generalized inverse filtering. However, inverse filtering is very sensitive to additive noise. The approach of reducing one degradation at a time allows us to develop a restoration algorithm for each type of degradation and simply combine them.

The Wiener filtering executes an optimal trade-off between inverse filtering and noise smoothing. It removes the additive noise and inverts the blurring simultaneously. The Wiener filtering is optimal in terms of the mean square error. In other words, it minimizes the overall mean square error in the process of inverse filtering and noise smoothing. The Wiener filtering is a linear estimation of the original image. The approach is based on a stochastic framework. The orthogonality principle implies that the Wiener filter in Fourier domain can be expressed as follows:

$$W(f_1, f_2) = \frac{H^*(f_1, f_2)S_{xx}(f_1, f_2)}{|H(f_1, f_2)|^2 S_{xx}(f_1, f_2) + S_{\eta\eta}(f_1, f_2)} \quad (1)$$

Where $S_{xx}(f_1, f_2)$, $S_{\eta\eta}(f_1, f_2)$ are respectively power spectra of the original image and the additive noise, and $H(f_1, f_2)$ is the blurring filter [8].

B. CURVELET TRANSFORM

Curvelets are based on multiscale ridgelets combined with a spatial bandpass filtering operation to isolate different scale. Like ridgelets, curvelets occur at all scales, locations, and orientations. However, while ridgelets all have global length and variable widths, curvelets in addition to a variable width have a variable length and so a variable anisotropy. The length and width at fine scales are related by a scaling law width \approx length² and so the anisotropy increases with decreasing scale like a power law. Recent work shows that thresholding of discrete curvelet coefficients provide near-optimal N -term representations of otherwise smooth objects with discontinuities along C^2 curves. Thus for understanding curvelet, we should knowledge about ridgelet and radon transform.

i) Continuous Ridgelet Transform

The ridgelet transform [3], [7] of two-dimensional function $f(x, y)$ allows the sparse representation of both smooth function and of straight edges by superposition of ridgelet function. For every $L^2(\mathbb{R}^2)$ we get its ridgelet coefficients $R_f(a, b, \theta)$ by a inner product with the frame like function $\Psi_{a, b, \theta}(x)$ which is a wavelet in transverse orientation constant along the line $x_1 \cos \theta + x_2 \sin \theta = \text{constant}$. For every $a > 0$, each $b \in \mathbb{R}$ and each $\theta \in [0, 2\pi)$, the bivariate ridgelet $\Psi_{a, b, \theta}$ is given by

$$\frac{1}{\sqrt{a}} \psi\left(\frac{x \cos \theta + y \sin \theta - b}{a}\right) \quad (2)$$

This function is constant along the lines $x_1 \cos \theta + x_2 \sin \theta = \text{constant}$. Transverse to these ridges it is a wavelet.

Given an integrable bivariate function $f(x)$, the ridgelet coefficients by

$$\mathcal{R}_f(a, b, \theta) = \int \psi_{a, b, \theta}(x) f(x) dx. \quad (3)$$

The reconstruction formulae is given as

$$f(x) = \int_0^{2\pi} \int_{-\infty}^{\infty} \int_0^{\infty} \mathcal{R}_f(a, b, \theta) \psi_{a, b, \theta}(x) \frac{da}{a^3} db \frac{d\theta}{4\pi} \quad (4)$$

The above equation (4) is valid for both integrable and square integrable. Furthermore, this formula is stable as one has a Parseval relation is given by



International Journal of Advanced Research in Electrical, Electronics and Instrumentation Engineering

(An ISO 3297: 2007 Certified Organization)

Vol. 3, Issue 1, January 2014

$$\int |f(x)|^2 dx = \int_0^{2\pi} \int_{-\infty}^{\infty} \int_0^{\infty} |\mathcal{R}_f(a, b, \theta)|^2 \frac{da}{a^3} db \frac{d\theta}{4\pi}. \quad (5)$$

Hence, much like the wavelet or Fourier transforms, the identity (5) expresses the fact that one can represent any arbitrary function as a continuous superposition of ridgelets.

ii) Radon Transform

A basic tool for calculating ridgelet coefficients is to view ridgelet analysis as a form of wavelet analysis in the Radon domain. The Radon transform of an object f is the collection of line integrals indexed by $(\theta, t) \in [0, 2\pi) \times \mathbb{R}$.

$$Rf(\theta, t) = \int f(x_1, x_2) \delta(x_1 \cos \theta + x_2 \sin \theta - t) dx_1 dx_2 \quad (6)$$

Where δ is the Dirac distribution. The ridgelet coefficients $R_f(a, b, \theta)$ of an object f are given by analysis of the Radon transform via

$$\mathcal{R}_f(a, b, \theta) = \int Rf(\theta, t) a^{-1/2} \psi((t - b)/a) dt. \quad (7)$$

Hence, the ridgelet transform [2] is precisely the application of a one-dimensional (1-D) wavelet transform to the slices of the Radon transform where the angular variable θ is constant and t is varying.

iii) Discrete Curvelet Transform of Continuum Function

The discrete curvelet transform [7] of a continuum function $f(x_1, x_2)$ makes use of a dyadic sequence of scales, and a bank of filters $\{[P]_0 f, \Delta_1 f, \Delta_2 f, \dots\}$ with the property that the pass band filter Δ_s is concentrated near the frequencies $[2^{2s}, 2^{2s+1}]$ e.g.

$$\Delta_s = \Psi_{2^s} * f, \quad \widehat{\Psi_{2^s}}(\xi) = \widehat{\Psi}(2^{-2s}\xi). \quad (8)$$

In wavelet theory, one uses decomposition into dyadic subbands $[2^s, 2^{s+1}]$. In contrast, the subbands used in the discrete curvelet transform of continuum functions have the nonstandard form $[2^{2s}, 2^{2s+1}]$. This is nonstandard feature of the discrete curvelet transform well worth remembering.

International Journal of Advanced Research in Electrical, Electronics and Instrumentation Engineering

(An ISO 3297: 2007 Certified Organization)

Vol. 3, Issue 1, January 2014

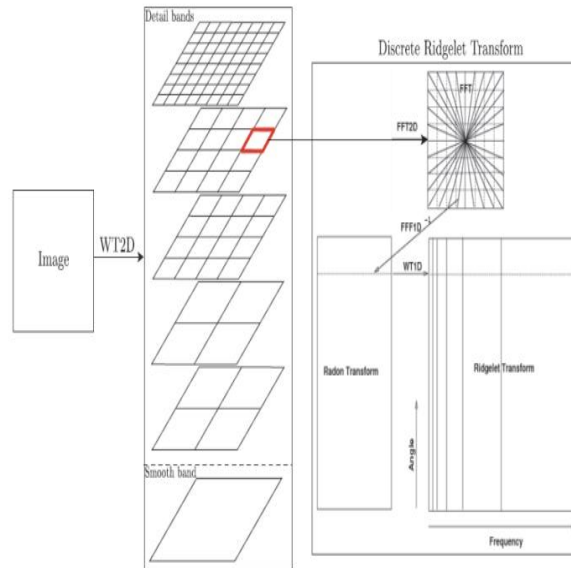


Fig.2. First Generation Discrete curvelet Transform (DCTG1) flowchart.

The Fig. 2 illustrates the decomposition of the original image into sub-bands followed by the spatial partitioning of each sub-band. The ridgelet transform [5] is then applied to each block.

The curvelet decomposition is the sequence of the following steps.

- *sub-band decomposition* : The object is decomposed into subbands (9)

$$f \mapsto (P_0 f, \Delta_1 f, \Delta_2 f, \dots).$$

- *Smooth Partitioning* : Each subband is smoothly windowed into “squares” of an appropriate scale (of side length $\sim 2^{-s}$) (10)

$$\Delta_s f \mapsto (w_Q \Delta_s f)_{Q \in \mathcal{Q}_s}.$$

- *Smooth Partitioning* : Each subband is smoothly windowed into “squares” of an appropriate scale (of side length $\sim 2^{-s}$) (11)

$$\Delta_s f \mapsto (w_Q \Delta_s f)_{Q \in \mathcal{Q}_s}.$$

- *Renormalization* : Each resulting square is renormalized to unit scale. (12)

$$g_Q = 2^{-s} (T_Q)^{-1} (w_Q \Delta_s f), \quad Q \in \mathcal{Q}_s.$$

- *Ridgelet Analysis* : Each square is analyzed in the ortho-ridgelet system. (13)

$$\alpha_\mu = \langle g_Q, \rho_\lambda \rangle, \quad \mu = (Q, \lambda).$$

In this definition, the two dyadic subbands $[2^{2s}, 2^{2s+1}]$ and $[2^{2s+1}, 2^{2s+2}]$ are merged before applying the ridgelet transform.

International Journal of Advanced Research in Electrical, Electronics and Instrumentation Engineering

(An ISO 3297: 2007 Certified Organization)

Vol. 3, Issue 1, January 2014

IV. PERFORMANCE CALCULATION

In this paper, we presented a strategy for denoising a noisy image by the wiener and the curvelet transforms. The noise level in an image can be estimated by calculating the PSNR value. Therefore, performance can be measured by comparing the PSNR values of the noisy, curvelet and the proposed algorithm. Mean Square Error is defined as:

$$MSE = \frac{1}{m \cdot n} \sum_{i=0}^{m-1} \sum_{j=0}^{n-1} [I(i,j) - K(i,j)]^2 \quad (14)$$

Where m, n represent number of rows and columns in the input image. I (i,j) and K (i,j) denotes the noise free and noisy pixel image respectively .

We used the peak signal-to-noise ratio (PSNR) measure to assess quality of the restored image and to compare the results quantitatively with previous filtering algorithms. The PSNR measure is defined as:

$$\begin{aligned} PSNR &= 10 \cdot \log_{10} \left(\frac{MAX_I^2}{MSE} \right) \\ &= 20 \cdot \log_{10} \left(\frac{MAX_I}{\sqrt{MSE}} \right) \\ &= 20 \cdot \log_{10} (MAX_I) - 10 \cdot \log_{10} (MSE) \end{aligned} \quad (15)$$

V. RESULT AND DISCUSSION

We test our algorithm with Peppers and Lena image. The tested images are corrupted with Gaussian white noise with noise standard deviation (σ) 10,20,30,40,50,60,70 respectively. The qualitative analysis of Peppers and Lena images, corrupted with White Gaussian noise, is shown in Fig. 3 and Fig. 5. The Peppers image corrupted with severe white Gaussian noise attack is demonstrated in Fig.3. Compare to curvelet algorithms, our proposed scheme highlights the best visible quality of the restored Peppers image. Table1 and 2 shows the simulation results, in terms of PSNR measure, for peppers and Lena standard images. In Table 1, our proposed scheme provided the best PSNR value for the Peppers image at various noise standard deviations. However, curvelet transform has given considerably low value. Fig. 4 and 6 shows the plot of PSNR values of proposed algorithm along with curvelet transform output and noisy image. We observed that the PSNR value of our proposed method is higher compare to curvelet transform and it works well for all the level of noises.

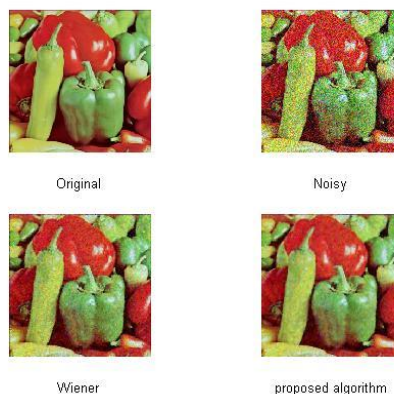


Fig.3. Peppers image with $\sigma = 40$ dB (a) original input image i.e. without noise, (b) image contaminated with white Gaussian noise, (c) Output image of Wiener filter, (d) output image of the proposed method.

International Journal of Advanced Research in Electrical, Electronics and Instrumentation Engineering

(An ISO 3297: 2007 Certified Organization)

Vol. 3, Issue 1, January 2014

TABLE 1. σ Vs PSNR value of peppers image.

σ (dB)	PSNR		
	Proposed algorithm in (dB)	Curvelet transform(dB)	Noisy image(dB)
10	36.4913	28.2318	28.1118
20	31.3377	22.3253	22.0901
30	28.1687	18.9076	18.5945
40	25.9377	16.4319	16.0804
50	24.0712	14.5199	14.1539
60	22.5495	12.9343	12.5663
70	21.3423	11.6289	11.2541

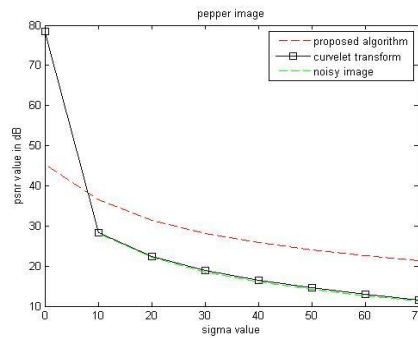


Fig.4. Plots the PSNR values of proposed algorithm along with curvelet transform output and noisy image.

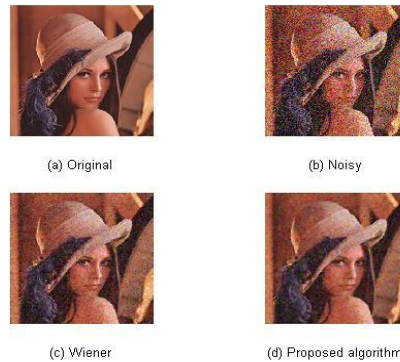


Fig.5. Lena image with $\sigma = 40$ dB (a) original input image i.e. without noise, (b) image contaminated with white Gaussian noise, (c) Output image of Wiener filter, (d) output image of the proposed method

TABLE 2. σ Vs PSNR value of Lena image.

σ (dB)	PSNR		
	Proposed algorithm (dB)	Curvelet transform(dB)	Noisy image(dB)
10	36.9005	28.2351	28.1175
20	31.5529	22.3884	22.1399
30	28.2837	18.8994	18.5744
40	26.0427	16.4484	16.0827
50	24.2623	14.5365	14.1599
60	22.6327	12.9518	12.5784
70	21.2731	11.6126	11.2468

International Journal of Advanced Research in Electrical, Electronics and Instrumentation Engineering

(An ISO 3297: 2007 Certified Organization)

Vol. 3, Issue 1, January 2014

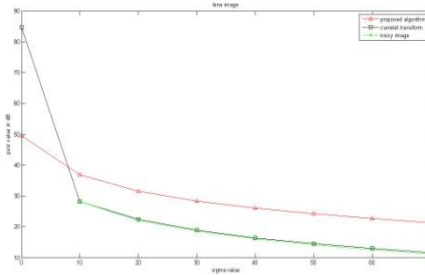


Fig.6. Plots the PSNR values of proposed algorithm along with curvelet transform output and noisy image.

V. CONCLUSION

Our proposed denoising algorithm has denoised pepper image and the PSNR value have been found to better than the curvelet and the wavelet transform. The algorithm performs even better in YCbCr region than in RGB region. The PSNR versus sigma graph has also been plotted which clearly explains that the proposed algorithm is more efficient. The graph shows a decrease in PSNR value as the sigma value increases, which is natural because, as the noise increases the signal to noise ratio is expected to decrease.

REFERENCES

- [1] Jean-Luc Starck, Emmanuel J. Candès, and David L. Donoho, "The Curvelet Transform for Image Denoising". IEEE Transactions on image processing, vol. 11, no. 6, June 2002.
- [2] A. Averbuch, R. R. Coifman, D. L. Donoho, M. Israeli, and J. Waldn" *Polar FFT, rectopolar FFT, and applications*, Stanford Univ., Stanford, CA, Tech. Rep., 2000.
- [3] E. J. Candès, "Harmonic analysis of neural networks," *Appl. Comput. Harmon. Anal.*, vol. 6, pp. 197–218, 1999.
- [4] Miller.M and Kingsbury, Nick "Image Denoising Using Derotated. Complex Wavelet Coefficients." IEEE Trans. Image Processing vol. 17, No.9, pp. 1500-1511, 2008.
- [5] Candès, E. J., "On the representation of mutilated Sobolev functions," Dept. Statist., Stanford Univ., Stanford, CA, Tech. Rep., 1999.
- [6] E. J. Candès and D. L. Donoho, "Curvelets—A surprisingly effective nonadaptive representation for objects with edges," in *Curve and Surface Fitting*. Nashville, TN: Vanderbilt Univ. Press, 1999.
- [7] A. Cohen, C. Rabut, and L. L. Schumaker, Eds., Nashville, "Ridgelets: The key to higher-dimensional intermittency?" *Phil. Trans. R. Soc. Lond. A.*, vol. 357, pp. 2495–2509, 1999.
- [8] M. Antonini, M. Barlaud, P. Mathieu, I. Daubechies, "Image coding using wavelet transform", IEEE Trans. Image Processing, Vol. 1, pp. 205-220, 1992.